Proceedings of ISFOG 2025
5TH INTERNATIONAL SYMPOSIUM ON
FRONTIERS IN OFFSHORE GEOTECHNICS
Nantes, France | June 9-13 2025

ISBN 978-2-85782-758-0

Pile sway calculation procedure and control during skirt pile driving operation in the North Sea

T. H. Tefera*
Aker Solutions AS, Oslo, Norway

B. Melhus
Aker Solutions AS, Oslo, Norway

S. Maghsoodi
Heerema Marine Contractors, Leiden, The Netherlands

S. Chenicheri Pulukul & S. Rose
Shell UK Limited, Aberdeen, UK

**tewodros.tefera@akersolutions.com*

ABSTRACT: This paper discusses the installation difficulties associated with driving long, slender piles that have minimal self-weight penetration. The most critical issue arises when pile sway occurs during installation, especially when driving begins with the heavy hammer positioned above or within the splash zone. Pile driving operations were performed to support a four-legged steel jacket in water depth of approximately 80m, consisting of four vertical skirt piles with a diameter of 2743mm (108") and 75.0m penetration. The total length of a single pile is 93.5m including stickup portion above mudline and the wall thickness varies between 75mm to 100mm. A submersible hydraulic hammer, IHC S2300, was used for the installation of the piles.

Pile sway occurs when the structural system comprising the pile and hammer or just the pile is exposed to a sea state with a given significant wave height and peak period. The assessment of pile sway to determine the dynamic response is performed through a spectral analysis. A set of sea states is exposed on the pile and hammer assembly. For each sea state and for different pile penetration depths, the most probable expected response is evaluated. The most probable extreme response typically occurs when the hammer is just above the still water level, i.e., predominantly in the splash zone. Experience from this installation demonstrates that the detailed pile sway analysis was an invaluable tool for monitoring and executing the pile installation that took place under a challenging weather condition.

Keywords: Pile sway; Offshore pile; Long pile; Wave loading.

1 INTRODUCTION

Pile driving operations were performed to support a four-legged steel jacket in water depth of approximately 80m, consisting of four vertical skirt piles with a diameter of 2743mm (108") and 75.0m penetration. The total length of a single pile is 93.5m including stickup portion above mudline and the pile wall thickness varies between 75mm to 100mm. Due to limited self-weight penetration, the piles are exposed to pile sway just after pile stabbing and during pile driving operation. Pile sway occurs when the structural system comprising the pile and hammer or just the pile is exposed to a sea state with a given significant wave height and peak period.

The effect of pile sway just after pile stabbing and during pile driving have been studied and monitored during pile driving operation. The assessment of pile sway to determine the response is performed through a spectral analysis. A set of sea states is exposed on the pile/hammer assembly and for each sea state and for each penetration depth, the most probable extreme response is evaluated assuming a Pierson-Moskowitz wave spectrum (Pierson and Moskowitz, 1964). The maximum extreme response typically occurs when the hammer is just above the still water level, i.e., predominantly in the splash zone. As the pile driving progresses, the pile/hammer assembly passes through this critical wave zone and eventually the response will be reduced. Both the maximum lateral displacement at top of the assembly as well as the maximum bending stress in the pile at the top spacer location in the pile sleeve are evaluated. The evaluation performed through the spectral analysis accounts for the dynamics and second order effects.

2 PLATFORM DESCRIPTION

The substructure of the platform is a four-legged, double symmetric with all faces battered steel jacket located in the central North Sea at a water depth of approximately 80.0m. The jacket supports the topside on top of the four legs and the foundation at the seabed consists of four vertical skirt piles with a diameter of 2743mm (108") and 75.0m penetration. The total length of a single pile is 93.5m including stickup portion above mudline and the wall thickness varies between 75mm to 100mm. Figure 1 and Figure 2 below show the jacket, excluding topside, with stabbed pile and with stabbed pile and hammer.

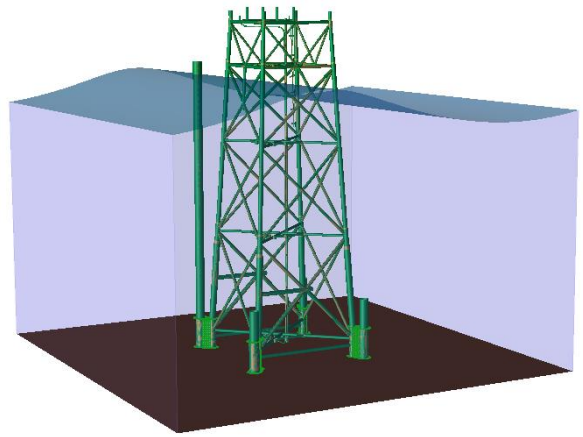

Figure 1. Model of the jacket with stabbed pile.

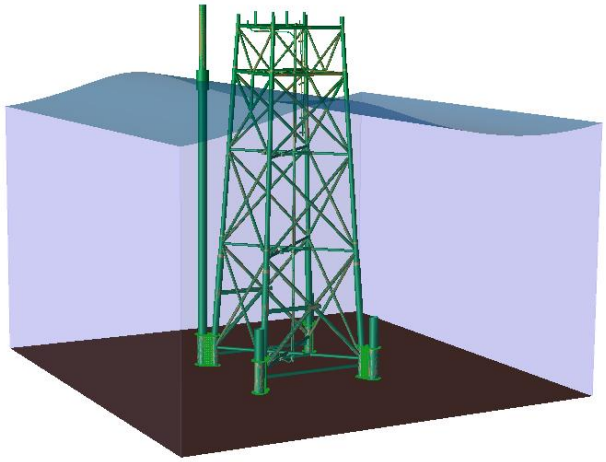

Figure 2. Model of the jacket with stabbed pile and hammer on top.

A submersible hydraulic hammer, IHC S2300, was used for the installation of the platform piles. Just after pile stabbing and during pile driving operation, the piles are exposed to pile sway. Hammer stabbing on top of stabbed pile is a very slow and careful operation. During hammer stabbing operation the vertical load due to hammer weight is the dominant load. The horzontal load due to hammer contact during hammer stabbing operation is very small compared to the wave load. The most critical issue arises especially when driving begins with the heavy hammer positioned above or within the splash zone. The two critical issues are hammer contact with the jacket structure and the utilization of the pile material due to dynamic bending stress at the upper pile spacer location in the pile sleeve. To ensure a safe pile installation operation the effects of pile sway during the pile driving operation must be understood. A detailed pile sway analysis was performed to determine the limiting sea state condition and permissible hammer energy.

3 PILE SWAY CALCULATION

3.1 Synopsis of theory

In the assessment of response due to pile sway a spectral analysis is performed and in the following a summary of the theoretical foundation is given assuming the pile is subjected to a given sea state. The pile may be modelled in any linear structural analysis software program that evaluates wave forces and dynamics. Subsequently, the geometry of the hammer along with its correct mass is applied on top of the pile. The kinematic factors (drag coefficient, Cd, and mass coefficent, Cm) may be set to Cd=0.65 and Cm=2.0 where the pile is assumed flooded.

A set of waves are then applied on to the pile and the static response, i.e. bending moment towards the pile sleeve and/or the displacement at top, is evaluated. To give a good description of the transfer function, the set of waves must constitute all relevant periods inherent in the wave spectrum. The wave steepness is set to 1/20 and hence for each period the wave height H is evaluated for a wave period T as shown in Equation 1 below where g is gravitational acceleration.

$$H = \frac{1}{20} \cdot \frac{g}{2.\pi} \cdot T^2 \quad (1)$$

The relevant sea state is modest, with significant wave heights $H_s \leq 6.0$m, and thus an ordinary Pierson-Moskowitz wave spectrum is assumed (Pierson and Moskowitz, 1964). The static response forms a continuous loading function $\sigma_0(\omega)$ where ω is the angular frequency of the wave.

The axial force along the pile, $N(z)$, is evaluated as shown in Equation 2.

$$N(z) = (M_h + (\rho_s - \rho_w) \cdot A_s(z) \cdot (L_c - z)) \cdot g \quad (2)$$

where M_h is the mass of the hammer, ρ_s and ρ_w are steel and water densities respectively, $A_s(z)$ is the cross-sectional area of the pile, L_c is length of the pile from seabed to center of gravity of hammer, CoG, and z is the distance from seabed. Note that N(z) is negative in compression. Subsequent account for buoyancy can be taken if needed. The generalized mass, m_G, is evaluated as shown in Equation 3.

$$m_G = \int_0^{L_c} m_p(z) \cdot \phi(\mathrm{z})^2 \, dz + M_h \cdot \phi(L_c)^2 \qquad (3)$$

where $m_p(z)$ is mass per unit length of the pile, including added mass and entrapped water. In lieu of other information the eigenvector of a cantilever is assumed as $\phi(\mathrm{z}) = 1 - \cos\left(\frac{\pi \cdot z}{2 \cdot L_c}\right)$. The generalized stiffness is evaluated as $k_o = \omega_0^2 \cdot m_G$, where $\omega_0 = \frac{2\pi}{T_0}$ and T_0 is the fundamental period as evaluated by the linear structural analysis software. The geometric stiffness, k_g, is evaluated as shown in Equation 4 below.

$$k_g = \int_0^{L_c} N(z) \cdot \left(\frac{d}{dz}\phi(\mathrm{z})\right)^2 dz \qquad (4)$$

The total effective stiffness becomes $k_2 = k_o + k_g$, accounting for geometric stiffness the updated fundamental period is then, $T_2 = 2\pi \cdot \sqrt{\frac{m_G}{k_2}}$.

The evaluated response (bending moment or displacement) is normalized to unit wave amplitudes, by dividing the response quantities by $H/2$, yielding a normalized version of the loading function $\sigma_0(\omega)$. Thereafter, the loading functions are adjusted to account for geometric stiffness as shown in Equation 5.

$$\sigma_2(\omega) = \sigma_0(\omega) \cdot \left(\frac{T_2}{T_0}\right)^2 \qquad (5)$$

The transfer function, $H(\omega)$, and the dynamic amplification factor, $DAF(\omega)$, as a function of angular frequency, ω, are shown in Equation 6 and 7.

$$H(\omega) = DAF(\omega) \cdot \sigma_2(\omega) \qquad (6)$$

$$DAF(\omega) = \frac{1}{\sqrt{\left(1-\left(\frac{\omega}{2\pi}T_2\right)^2\right)^2 + 4.0 \cdot \xi^2 \cdot \left(\frac{\omega}{2\pi}T_2\right)^2}} \qquad (7)$$

The damping ratio is set to $\xi = 0.02$. The response spectrum, $S_r(\omega)$, and its zeroth and second spectral moments are expressed as shown in Equation 8, 9, and 10.

$$S_r(\omega) = H(\omega)^2 \cdot S_p(\omega) \qquad (8)$$

$$m_0 = \int_{\omega_l}^{\omega_u} S_r(\omega) \cdot d\omega \qquad (9)$$

$$m_2 = \int_{\omega_l}^{\omega_u} \omega^2 \cdot S_r(\omega) \cdot d\omega \qquad (10)$$

Where $S_p(\omega)$ is the wave spectrum, ω_l and ω_u are the cut-off frequencies. The mean upcrossing period of the response is calculated as $T_{zr} = 2\pi \cdot \sqrt{\frac{m_0}{m_2}}$.

Finally, the most probable extreme response of either bending moment or displacement is calculated using extreme value theory and expressed as shown in Equation 11.

$$\sigma_{max} = \frac{1}{2} \cdot \sqrt{m_0} \cdot \ln\left(\frac{T_S}{T_{zr}}\right)^{\frac{1}{\beta}} \cdot \alpha^{\frac{1}{\beta}} \qquad (11)$$

where T_S is the sea state duration, i.e. T_S = 3 hours. Given the narrowbandness of the response, i.e. a Rayleigh distribution is appropriate, the Weibull parameters can be taken as $\alpha = 8$ and $\beta = 2$. The above calculations are performed for a series of sea states, defined by a specified maximum allowable significant wave height H_S and a range of probable peak periods T_P. Normally, maximum response is obtained close to the fundamental period T_2. In cases where this fundamental period is outside existing peak periods of the scatter diagram, the limiting value of the peak period will produce the maximum response. In lieu of other information this lower peak period of the scatter diagram can be taken as in Equation 12 according to DNV recommended practice (DNV-RP-N103, 2021).

$$T_{p\_min} = 12.46 \cdot \sqrt{\frac{H_S}{9.81}} \qquad (12)$$

3.2 Extreme value analysis

Following the procedure as outlined in Section 3.1 an extreme value analysis is performed on pile sway. In the assessment, IHC S2300 submersible hydraulic hammer with total dry weight of M_h= 392tonne is used. The sea states evaluated have significant wave heights in the range of Hs = 1.0m to 4.0m with peak periods in the range of Tp = 4.0sec. to 18.9sec. For the scenario with stabbed pile only, excluding the hammer, the sea states Hs of 2.5m, 4.5m and 5.7m are checked. The most probable extreme bending moment including the secondary effect due to the mass of hammer, M_{max}, at the upper spacer location is

evaluated. M_{max} in accordance with NORSOK standards, must incorporate an environmental load factor of γ=1.3. Subsequently a capacity check in accordance with NORSOK is evaluated as shown in Equation 13 (NORSOK N-004, 2022).

$$\frac{N_{sd}}{N_{cl,Rd}} + \frac{M_{max}}{M_{Rd}} \leq 1.0 \qquad (13)$$

where $N_{cl,Rd}$ and M_{Rd} are design axial local buckling resistance and design bending resistance respectively and are calculated from the cross-sectional parameters of the pile. N_{sd} is the design axial compression force, encompassing the deadweight exerted by the pile above the upper spacer location in the pile sleeve and the hammer. Additional load due to hammer energy during pile driving is also included in N_{sd}.

4 PILE SWAY ASSESSMENT

During the pile installation operation, the piles are first lifted and stabbed in the pile sleeves. The pile self-weight penetration in the seabed depends on the seabed soil condition and the pile weight. Based on the pile weight and hammer weight the pile self-weight penetration is calculated using SRD values. The calculated self-weight penetration for pile only is 3.1m to 3.7m and with hammer on top of pile is from 4.5m to 5.3m. The pile inside the pile sleeve is supported by pile spacers located at the bottom and top part of the pile sleeve. The lateral displacement of the pile and the dynamic bending stress response in the pile at the upper pile spacer location due to various sea states have been calculated according to the procedure described in Section 3. The analysis performed is to check two conditions during pile installation operation. The first condition is any contact between the stabbed pile and the jacket structure, and between the hammer on top of the pile during pile driving and the jacket structure. The clearance check is performed for different sea states and pile penetration depths. The second condition is the utilization of the pile limiting bending moment capacity for different sea states and the pile penetration depths. Figure 1 and Figure 2 show the two scenarios checked, stabbed pile only and stabbed pile with hammer on the pile.

4.1 Stabbed pile only

The dynamic bending stress response of the stabbed pile, without hammer on top of the pile at the upper pile spacer location under various sea states, has been calculated with a load factor of 1.3 and a material factor of 1.15 (NORSOK N-004, 2022). The induced bending stress in the pile due to wave load, i.e. the dynamic bending stress in the pile at the upper pile spacer location in the pile sleeve, as a function of sea state and peak wave period are shown in Figure 3. This figure shows the dynamic bending stress as a function of significant wave heights, Hs, and peak wave periods, Tp. The pile bending stress capacity at the contact point of the upper pile spacer and the pile in the pile sleeve is also shown in Figure 3. As shown in the figure, the pile has sufficient capacity for the induced dynamic bending moment for the significant wave hights up to Hs = 5.7m. Note that the lower peak wave period increases with the specific wave heights.

The corresponding lateral displacement at the top of the pile as function of Hs and Tp is shown in Figure 4. A 3D clearance check with the jacket structure is shown in Figure 5.

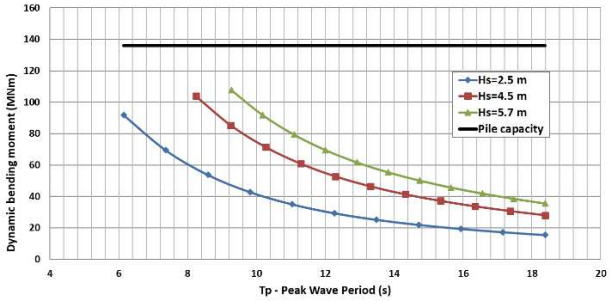

Figure 3. Dynamic bending stress response, stabbed pile.

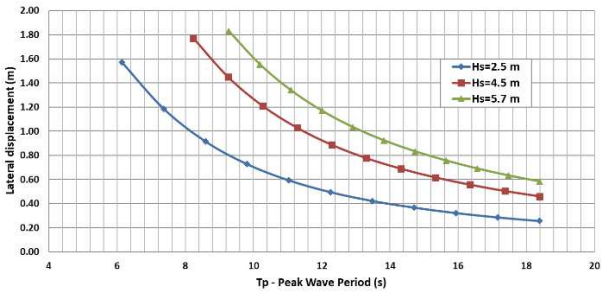

Figure 4. Top of pile lateral displacement, stabbed pile.

The analysis for the stabbed pile case without hammer show that the pile has sufficient capacity for the induced dynamic bending moment due to wave load and the pile has sufficient clearance with the jacket structures.

4.2 Stabbed pile with hammer on top

The most probable extreme response of the system typically occurs when the bigger geometry of the system, in this case the hammer, is close to the splash zone. Figure 6 below shows stabbed pile and hammer on top of stabbed pile during pile driving. The figure shows the hammer is close to splash zone before it is submerged and exposed to the wave load. As the pile

penetrates more into the seabed, the pile stickup is shorter, and this reduces the pile sway effect.

Figure 5. Clearance check for stabbed pile only with jacket structure for sea state of Hs=5.7m.

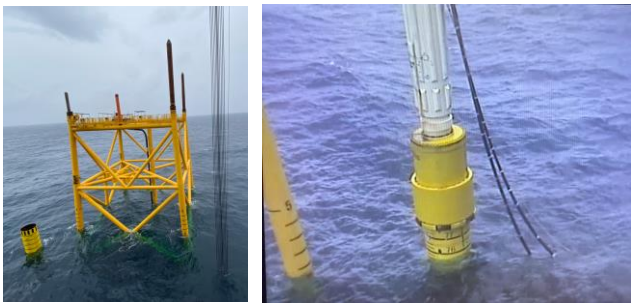

Figure 6. Jacket with stabbed pile and with hammer on stabbed pile.

The induced bending stress in the pile due to wave load, i.e. the dynamic bending stress in the pile at the upper spacer location in the pile sleeve as a function of sea state and peak wave period is shown in Figure 7.

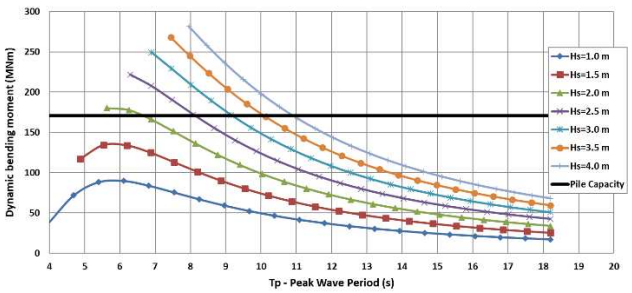

Figure 7. Dynamic bending stress response at the critical pile penetration depth.

Figure 7 shows the calculated dynamic bending stress response at the critical pile penetration depth when the hammer is in the splash zone. As shown in the figure, for a critical peak wave period, Tp≤ 6.5sec, the pile does not have sufficient capacity for sea states of Hs ≥ 2.0m. Note that to apply hammer energy for pile driving, sufficient reserve pile capacity is needed. The corresponding lateral displacement at the hammer center of gravity, CoG, location as a function of sea state and peak wave period at the critical pile penetration depth is shown in Figure 8. The analysis for the stabbed pile with hammer on top shows that the pile has sufficient clearance with the jacket structures. However, the pile has limited capacity for the induced dynamic bending moment due to wave load for the critical peak wave periods. Furthermore, the pile does not have reserve capacity for the additional induced stress from applied hammer operating energy. The hammer operating energy is the required hammer energy for that penetration level to overcome the soil resistance under 'reasonable' blow count values. To calculate the additional induced stress in the pile due to the applied hammer operating energy, the wave equation analysis program GRLWEAP has been used (Pile Dynamic Inc., 2014).

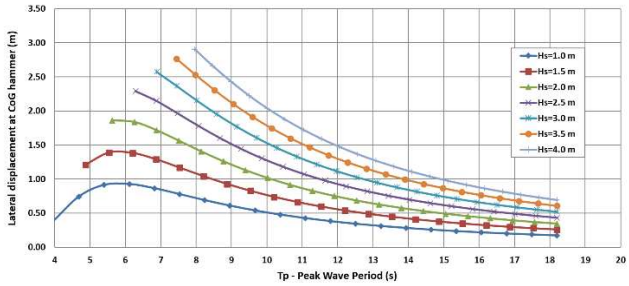

Figure 8. Lateral displacement at CoG location of the hammer.

5 PILE DRIVING OPERATION

The significant wave height, Hs, for the most probable expected maximum sea state in the installation window is 5.7 m. In this installation window, the jacket fulfils the on bottom stability requirements. The on bottom stability analysis also shows maximum two piles stabbed can fulfil the on bottom stability requirements. Therefore, the pile driving operation is planned to stab and drive piles in two batches of two piles. A wave rider buoy was deployed throughout the operation to provide real-time sea state information.

5.1 Pile stabbing and visual observation

The operation of pile driving commences with stabbing of two of the skirt piles. After the piles were stabbed, the weather condition deteriorated slightly. Before proceeding with stabbing the hammer on top of the pile, lateral displacement monitoring of the stabbed piles was performed.

Figure 9. The first batch of two stabbed piles and a close view of one of the piles during pile movement monitoring.

Figure 9 shows the first batch of two stabbed skirt piles. Monitoring the lateral displacement of these piles show the predicted lateral displacement due to pile sway is in good agreement with the actual sea state condition.

5.2 Pile driving and monitoring

During pile driving operation the applied hammer energy is restricted by the reserve pile capacity. The reserve pile capacity is the pile capacity at a given pile penetration depth minus the mobilized dynamic bending moment due to pile sway. The permissible hammer energy is calculated based on the reserve pile capacity using the wave equation analysis program GRLWEAP. The permissible hammer energy is required to overcome the SRD. Figure 10 shows the reserve pile capacities for significant wave heights of, Hs = 1.5m.

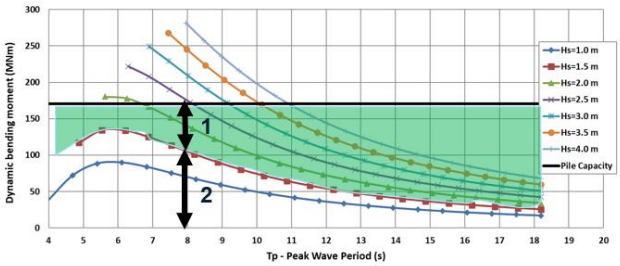

Figure 10. The green area shows the reserve pile capacity for additional load due to hammer energy for Hs=1.5m

In Figure 10 the reserve pile capacities rage at different wave periods is different as shown by arow 1. This section, arow 1, is the stress induced by hammer blows. The section shown by arow 2 is the stress contribution from metocean conditions induced sway and stresses from 2nd order moment of deadweight.

As described in Section 4, there is a direct link between the induced dynamic bending moment and lateral displacement due to pile sway. To monitor the pile driving operations a survey prism was installed at the top of the hammer to measure the lateral displacements. Figure 11 shows a picture from the observation screen. In the figure, the centre of the cercle is position of the hammer with no lateral displacement or tilt of pile.

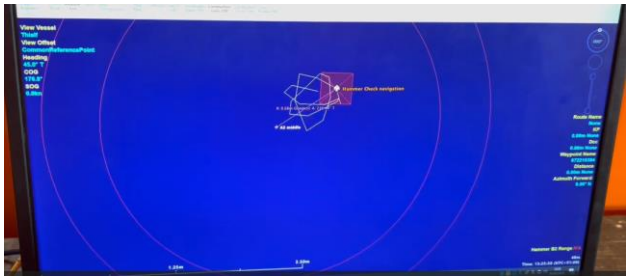

Figure 11. Traces of the hammer top movement during pile driving operation.

Traces of the hammer top movement during pile driving operation shown in Figure 11 relative to the centre of the circle is shown in Figure 12. The measurement data shown in Figure 11 and Figure 12 show the tilt at the top of the hammer is about 0.41m.

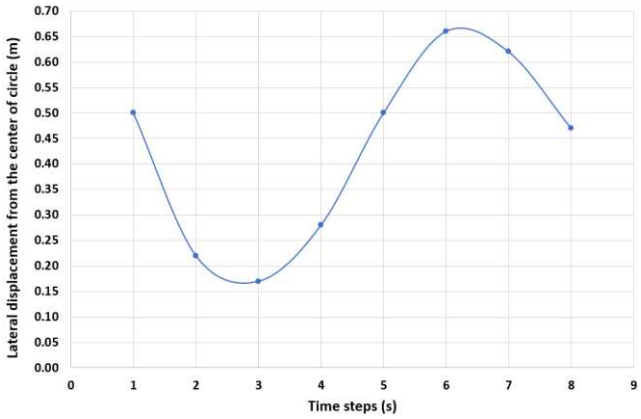

Figure 12. Traces of the hammer top movement during pile driving operation shown in Figure 11 relative to the centre of the circle.

Based on the lateral displacement at the hammer top two limits of lateral displacement for pile driving were established. The first limit indicates a safe driving operation with permissible hammer energy. Displacement between the first and the second limit indicates to keep the hammer on top of the pile without

applying hammer energy. When the lateral movement approaches the second limit, the lateral displacement is excessive then the hammer needs to be retrieved. Note that during pile driving operation the hammer is attached to the hook continuously, hence, retrieving the hammer is rather quick operation.

6 CONCLUSIONS

This paper discusses the installation challenges associated with driving long, slender piles. The most critical issue arises when pile sway occurs during installation. The pile sway assessment performed through the spectral analysis accounts for the dynamics and second order effects. The most probable extreme response typically occurs when the hammer is just above the still water level, i.e., predominantly in the splash zone. Based on the lateral displacement at the hammer top, two limits of lateral displacement were established as a tool during pile driving operations. The established limits are for safe driving with permissible hammer energy and to keep the hammer on top of the pile without applying hammer energy or retrieve the hammer. This tool prepared to follow the pile installation operation was a useful tool for monitoring and executing the pile installation that took place under a challenging weather condition.

The measured data during pile installation operation show good agremment with the calaculated data. Considering pile clerances in the pile sleeve and fabrication tolerances a maximum tilt at the top of hammer was calculated to be 0.96m. The measured tilt at the start of driving was about 0.41m. The actual self-weght penetration was slightly higher than the predicted self-weght penetration. The predicted lateral displacement for the sea stae during pile installtion operation was between 0.50m and 1.39m. The observed maximum was 0.65m.Author contribution statement

First Author: Pile sway assessment, writing-reviewing and editing. **Second Author**: Pile sway theory and calculation procedure, writing- reviewing. **Third Author**: Offshore monitoring and reviewing. **Fourth and Fifth Authors**: Client representatives and reviewers.

ACKNOWLEDGEMENTS

The authors are grateful for the permission to publish these data to Shell UK Limited. The authors would like to thank Aker Solutions AS for providing the resources for writing this paper. The authors would like also to thank Hannah J. Melhus and Pål R. Hovind from Aker Solutions AS for performing numerous analyses using the proposed calculation procedure and confirming its excellent agreement with time series simulations.

REFERENCES

NORSOK N-004 (2022). Design of offshore structures. The Norwegian continental shelf and comprise petroleum industry standards in Norway.

DNV – RP - N103 (2021). Modelling and analysis of marine operations.

Pile Dynamic Inc. (2014). GRLWEAP, Wave Equation Analysis of Pile Driving. Procedures and Models, Version 2014.

Pierson, Willard J., Jr. and Moskowitz, Lionel A. Proposed Spectral Form for Fully Developed Wind Seas Based on the Similarity Theory of S. A. Kitaigorodskii, *Journal of Geophysical Research*, Vol. 69, p.5181-5190, 1964.